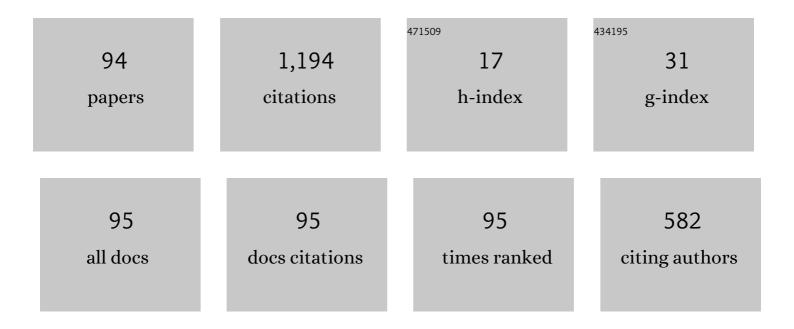
Hirotsugu Yamamoto

List of Publications by Year in descending order

Source: https://exaly.com/author-pdf/7853693/publications.pdf Version: 2024-02-01



#	Article	IF	CITATIONS
1	Improvement of apparent resolution by subjective super-resolution display for aerial display using AIRR. Optical Review, 2022, 29, 241-249.	2.0	3
2	Improvement of the distortion of aerial displays and proposal for utilizing distortion to emulate three-dimensional aerial image. Optical Review, 2022, 29, 261-266.	2.0	3
3	Examination of deblur processing according to optical parameters in aerial image. , 2022, 1, 462.		3
4	Pâ€57: <i>Student Poster:</i> Improved Modulation Transfer Function (MTF) for Aerial Image Formed with AIRR by Use of Two Transparent Spheres. Digest of Technical Papers SID International Symposium, 2022, 53, 1257-1260.	0.3	2
5	Theoretical and Experimental Perceived Depths in Arc 3D Displays: On/Off Switching Using Liquid-Crystal Active Devices. IEEE Industry Applications Magazine, 2021, 27, 69-81.	0.4	3
6	Full-field fluorescence lifetime dual-comb microscopy using spectral mapping and frequency multiplexing of dual-comb optical beats. Science Advances, 2021, 7, .	10.3	14
7	Influence of incident angle, anisotropy, and floating distance on aerial imaging resolution. OSA Continuum, 2021, 4, 865.	1.8	9
8	Reduction of retro-reflector and expansion of the viewpoint of an aerial image by the use of AIRR with transparent spheres. OSA Continuum, 2021, 4, 1207.	1.8	10
9	Proposal of moire-free aerial display based on the LED panel and apertured retro-reflector. Optical Review, 2021, 28, 492-500.	2.0	2
10	Multicascade-linked synthetic-wavelength digital holography using a line-by-line spectral-shaped optical frequency comb. Optics Express, 2021, 29, 15772.	3.4	2
11	High-speed driving of multi-color LED panel for subjective super-resolution display. Optical Review, 2021, 28, 508-515.	2.0	0
12	Edge-Based DFD (Depth-Fused 3-D) Display With Enlarged Viewing Angle and Maximum Perceived Depth. IEEE Transactions on Industry Applications, 2020, 56, 7193-7201.	4.9	1
13	Optical image amplification in dual-comb microscopy. Scientific Reports, 2020, 10, 8338.	3.3	6
14	Roadmap on 3D integral imaging: sensing, processing, and display. Optics Express, 2020, 28, 32266.	3.4	105
15	Aerial image resolution measurement based on the slanted knife edge method. Optics Express, 2020, 28, 35518.	3.4	16
16	Triple-views aerial display to show different floating images for surrounding directions. Optics Express, 2020, 28, 35540.	3.4	12
17	Multiple aerial imaging by use of infinity mirror and oblique retro-reflector. Japanese Journal of Applied Physics, 2020, 59, SOOD08.	1.5	16
18	Reducing Aberration of Aerial Image by Use of Supporting Wire in Large Aerial Display with AIRR. Proceedings of the International Display Workshops, 2020, , 715.	0.1	1

#	Article	IF	CITATIONS
19	Projecting a flat plane to a spherical surface by use of a compensation mirror. Optical Review, 2019, 26, 411-421.	2.0	1
20	Development of omnidirectional aerial display with aerial imaging by retro-reflection (AIRR) for behavioral biology experiments. Optical Review, 2019, 26, 221-229.	2.0	22
21	Aerial depth-fused 3D image formed with aerial imaging by retro-reflection (AIRR). Optical Review, 2019, 26, 179-186.	2.0	22
22	Theoretical and Experimental Perceived Depths in Arc 3D Display and Its On/Off Switching Using Liquid-Crystal Active Devices. , 2019, , .		1
23	Edge-Based DFD (Depth-Fused 3D) Display with Enlarged Viewing Angle & Maximum Perceived Depth. , 2019, , .		1
24	Scan-Less, Kilo-Pixel, Line-Field Confocal Phase Imaging with Spectrally Encoded Dual-Comb Microscopy. IEEE Journal of Selected Topics in Quantum Electronics, 2019, 25, 1-8.	2.9	1
25	Refractive index sensing with temperature compensation by a multimode-interference fiber-based optical frequency comb sensing cavity. Optics Express, 2019, 27, 21463.	3.4	19
26	Visualization of internal structure and internal stress in visibly opaque objects using full-field phase-shifting terahertz digital holography. Optics Express, 2019, 27, 33854.	3.4	8
27	Ultrasonic wave sensing using an optical-frequency-comb sensing cavity for photoacoustic imaging. OSA Continuum, 2019, 2, 439.	1.8	6
28	Lock-in-detection dual-comb spectroscopy. OSA Continuum, 2019, 2, 1998.	1.8	5
29	Subjective Super-Resolution Model on Coarse High-Speed LED Display in Combination with Pseudo Fixation Eye Movements. IEICE Transactions on Electronics, 2019, E102.C, 780-788.	0.6	2
30	Spatio-Temporal LED Driving for Subjective Super-Resolution of Grayscale Images. Proceedings of the International Display Workshops, 2019, , 1243.	0.1	2
31	Exploring the combination of optical components suitable for the large device to form aerial image by AIRR. Proceedings of the International Display Workshops, 2019, , 1382.	0.1	3
32	Lens-less fiber coupling of a 1550-nm mode-locked fiber laser light on a low-temperature-grown GaAs photoconductive antenna. OSA Continuum, 2019, 2, 1310.	1.8	0
33	Aquatic information display and its applications for behavioral biology experiments. , 2019, , .		1
34	Aerial Display on a Clear Sphere with Aerial Imaging by Retro-Reflection. , 2019, , .		1
35	The Trend of Three Dimensional Image Technology. Kyokai Joho Imeji Zasshi/Journal of the Institute of Image Information and Television Engineers, 2019, 73, 90-95.	0.1	0
36	Real-Time Amplitude and Phase Imaging of Optically Opaque Objects by Combining Full-Field Off-Axis Terahertz Digital Holography with Angular Spectrum Reconstruction. Journal of Infrared, Millimeter, and Terahertz Waves, 2018, 39, 561-572.	2.2	22

HIROTSUGU YAMAMOTO

#	Article	IF	CITATIONS
37	Strain sensing based on strain to radio-frequency conversion of optical frequency comb. Optics Express, 2018, 26, 9484.	3.4	20
38	Scan-less confocal phase imaging based on dual-comb microscopy. Optica, 2018, 5, 634.	9.3	70
39	Refractive-index-sensing optical comb based on photonic radio-frequency conversion with intracavity multi-mode interference fiber sensor. Optics Express, 2018, 26, 19694.	3.4	30
40	Multicascade-linked synthetic wavelength digital holography using an optical-comb-referenced frequency synthesizer. Optics Express, 2018, 26, 26292.	3.4	16
41	Forming aerial 3D images with smooth motion parallax in combination of arc 3D display with AIRR. , 2018, , .		0
42	2. Aerial Multi-modal Display. Kyokai Joho Imeji Zasshi/Journal of the Institute of Image Information and Television Engineers, 2018, 72, 488-491.	0.1	0
43	29â€1: An Aerial Display: Passing through a Floating Image Formed by Retroâ€Reflective Reimaging. Digest of Technical Papers SID International Symposium, 2017, 48, 406-409.	0.3	4
44	Aerial light-field image augmented between you and your mirrored image. , 2017, , .		4
45	Multifunctional aerial display through use of polarization-processing display. Optical Review, 2017, 24, 72-79.	2.0	14
46	Scan-less hyperspectral dual-comb single-pixel-imaging in both amplitude and phase. Optics Express, 2017, 25, 21947.	3.4	46
47	Comparison of Divergence Angle of Retro-Reflectors and Sharpness with Aerial Imaging by Retro-Reflection (AIRR). IEICE Transactions on Electronics, 2017, E100.C, 958-964.	0.6	12
48	4320-Hz LED Display With Pulse-Width Modulation by Use of a Nonlinear Clock. Journal of Display Technology, 2016, 12, 1581-1587.	1.2	6
49	Real-Time Determination of Absolute Frequency in Continuous-Wave Terahertz Radiation with a Photocarrier Terahertz Frequency Comb Induced by an Unstabilized Femtosecond Laser. Journal of Infrared, Millimeter, and Terahertz Waves, 2016, 37, 473-485.	2.2	2
50	Enlargement of Continuous Perceived Depth Region in Depth-fused 3-D Display. IEEE Transactions on Industry Applications, 2016, 52, 5226-5230.	4.9	2
51	Terahertz Frequency-Domain Spectroscopy of Low-Pressure Acetonitrile Gas by a Photomixing Terahertz Synthesizer Referenced to Dual Optical Frequency Combs. Journal of Infrared, Millimeter, and Terahertz Waves, 2016, 37, 903-915.	2.2	16
52	Brightness improvement by polarization modulation in the aerial imaging by retro-reflection (AIRR). , 2016, , .		2
53	Immersive 3D Environment by Floating Display and High-speed Gesture UI Integration. Transactions of the Society of Instrument and Control Engineers, 2016, 52, 134-140.	0.2	3

54 R2D2 w/ AIRR. , 2015, , .

HIROTSUGU YAMAMOTO

#	Article	IF	CITATIONS
55	Different aerial image formation into two directions by crossed-mirror array. Optical Review, 2015, 22, 862-867.	2.0	6
56	Adaptive sampling dual terahertz comb spectroscopy using dual free-running femtosecond lasers. Scientific Reports, 2015, 5, 10786.	3.3	60
57	Evaluation methods of retro-reflector for polarized aerial imaging by retro-reflection. , 2015, , .		7
58	Photographing-decodable steganography by use of a high-frame-rate LED display. , 2015, , .		0
59	Real-time absolute frequency measurement of continuous-wave terahertz radiation based on dual terahertz combs of photocarriers with different frequency spacings. Optics Express, 2015, 23, 11367.	3.4	31
60	Floating aerial LED signage based on aerial imaging by retro-reflection (AIRR). Optics Express, 2014, 22, 26919.	3.4	139
61	62.3: Handâ€Waving Steganography by Use of a Highâ€Frameâ€Rate LED Panel. Digest of Technical Papers SID International Symposium, 2014, 45, 915-917.	0.3	3
62	Edge-Based Depth-Fused 3D Display. , 2013, , .		3
63	A new method to enlarge a range of continuously perceived depth in DFD (depth-fused 3D) display. Proceedings of SPIE, 2013, , .	0.8	5
64	Aerial 3D LED display by use of retroreflective sheeting. Proceedings of SPIE, 2013, , .	0.8	19
65	64.3L: <i>Lateâ€News Paper</i> : Aerial Imaging by Retroâ€Reflection (AIRR). Digest of Technical Papers SID International Symposium, 2013, 44, 895-897.	0.3	16
66	Hand-waving decodable steganography by use of 960Hz LED panel. , 2013, , .		1
67	Perceived Depth Change Produced by Visual Acuity Difference between the Eyes. IEICE Transactions on Electronics, 2012, E95.C, 1707-1715.	0.6	13
68	111534 DNA scaffold logic : logic operation on molecular inputs using FRET cascades(Bioinformatics) Tj ETQq0 0 Seibutsu Butsuri, 2012, 52, S36.	0 rgBT /Ov 0.1	verlock 10 Tf 0
69	Experimental investigation of the closest parallel pulses in holographic femtosecond laser processing. Applied Physics A: Materials Science and Processing, 2012, 107, 357-362.	2.3	23
70	Viewing-Zone Control of Light-Emitting Diode Panel for Stereoscopic Display and Multiple Viewing Distances. Journal of Display Technology, 2010, 6, 359-366.	1.2	14
71	Visual Cryptography Using Polarization-Modulation Films. Japanese Journal of Applied Physics, 2009, 48, 09LC02.	1.5	11
72	Photon-counting digital holography under ultraweak illumination. Optics Letters, 2009, 34, 1081.	3.3	28

Hirotsugu Yamamoto

#	Article	IF	CITATIONS
73	Depth perception for moving images shown on a large LED display with an aperture grille. Journal of the Society for Information Display, 2009, 17, 1031-1036.	2.1	4
74	Manually operated low-coherence interferometer for optical information hiding. Optics Express, 2006, 14, 9421.	3.4	5
75	Near-Infrared Spectroscopy Probe with Position Sensor. Optical Review, 2005, 12, 149-154.	2.0	1
76	Secure Information Display with Two Limited Viewing Zones Using Two Decoding Masks Based on Visual Secret Sharing Scheme. Japanese Journal of Applied Physics, 2005, 44, 1803-1807.	1.5	13
77	Three-dimensional optical memory using a human fingernail. Optics Express, 2005, 13, 4560.	3.4	12
78	Optical image processing using an optoelectronic feedback system with electronic distortion correction. Optics Express, 2005, 13, 4657.	3.4	4
79	Optical Bit Recording in a Human Fingernail. Japanese Journal of Applied Physics, 2004, 43, 168-171.	1.5	10
80	Processing Structures on Human Fingernail Surfaces Using a Focused Near-Infrared Femtosecond Laser Pulse. Japanese Journal of Applied Physics, 2004, 43, 8089-8093.	1.5	13
81	Secure information display with limited viewing zone by use of multi-color visual cryptography. Optics Express, 2004, 12, 1258.	3.4	42
82	Flow of optical patterns due to small lateral wave-front shifts in a nonlinear optical feedback system. Optics Communications, 2003, 220, 281-287.	2.1	2
83	Securing information display by use of visual cryptography. Optics Letters, 2003, 28, 1564.	3.3	51
84	Spatially localized states with size-dependent optical bistability. Optics Letters, 2003, 28, 2351.	3.3	3
85	Thick photorefractive polymer device with coplanar electrodes. Review of Scientific Instruments, 2003, 74, 3693-3696.	1.3	4
86	Stereoscopic Full-Color Light Emitting Diode Display Using Parallax Barrier for Different Interpupillary Distances. Optical Review, 2002, 9, 244-250.	2.0	16
87	Spatial and Temporal Properties of a Nonlinear Optical Feedback System. Optical Review, 2001, 8, 343-347.	2.0	8
88	Selection of optical patterns using direct modulation method of spatial frequency in a nonlinear optical feedback system. Optics Communications, 2001, 187, 49-55.	2.1	11
89	Efficiency characteristics of linear dc motor by using a novel measuring method. Sensors and Actuators A: Physical, 2001, 91, 137-140.	4.1	6
90	Spatial Property of Formed Patterns Depending on Focus Condition in a Two-Dimensional Optoelectronic Feedback System. Japanese Journal of Applied Physics, 2001, 40, 165-169.	1.5	3

#	Article	IF	CITATIONS
91	Optical dependence of spatial frequency of formed patterns on focusing deviation in a nonlinear optical ring resonator. Optics Communications, 1998, 151, 263-267.	2.1	18
92	Iron deposits in the human labial minor salivary glands: A postmortem study The Journal of Nihon University School of Dentistry, 1989, 31, 361-365.	0.1	4
93	Acute symmetrical ulcers in the pyloric antrum of the stomach. Gastroenterologia Japonica, 1972, 7, 360-360.	0.3	0
94	Aerial imaging steganography method for aerial imaging by retro-reflection with dual acrylic ball. Optical Review, 0, , 1.	2.0	3